Published in the International Journal of Greenhouse Gas Control

Density measurements and modelling of loaded and unloaded aqueous solutions of MDEA (N-Methyldiethanolamine), DMEA(N,N-Dimethylethanolamine), DEEA (Diethylethanolamine) and MAPA (N-Methyl-1,3-diaminopropane)

Diego D. D. Pinto[1], Juliana G. M.-S. Monteiro[1], Birgit Johnsen[1], Hallvard F. Svendsen[1], Hanna Knuutila[1,*]

[1]Department of Chemical Engineering, Norwegian University of Science and Technology, N-7491 Trondheim, Norway

[*] Corresponding author: hanna.knuutila@.ntnu.no

Phone: +47 735 94119

Address: Sem Sælands vei 6

Department of Chemical Engineering

Norwegian University of Science and Technology

7491 Trondheim

Keywords: Density, Redlich-Kister, Rackett, Proportionality model, CO_2 capture

1. Introduction

Chemical absorption is well established as a benchmark technology for acid gas removal and carbon capture. Many amine solvents are being developed in order to reduce the energy requirements of the process, mainly associated with the heat needed in the regeneration part of the plant. In order to design absorption and desorption towers several properties of the chemical system must be accurately calculated using models based on experimental data. The most important experimental data are CO_2 solubility, kinetic constants and physical properties such as density and viscosity (Mokraoui et al., 2006).

Densities for unloaded amine solutions have been widely studied and data are available in the literature for several amines in a comprehensive range of temperatures and compositions. However, many different models have been proposed to correlate the experimental data. Cheng et al. (1996) proposed an empirical correlation using 7 parameters for estimation of MEA density. Zhang et al. (1995) used the Redlich-Kister

equation with up to 11 parameters for each temperature to correlate density, while Hartono and Svendsen (2009) and Han et al. (2012b) used 6 and 4 Redlich-Kister parameters respectively. Furthermore, Hartono and Svendsen (2009) introduced a linear temperature dependency to the Redlich-Kister parameters, allowing for density estimations over the whole range of compositions and temperatures by fitting a total of 12 parameters (since each Redlich-Kister parameter is described by 2 parameters). Han et al. (2012a) adopted the same strategy and was therefore able to calculate densities by fitting a total of 8 parameters.

In the present work the densities of aqueous solutions of MDEA (N-Methyldiethanolamine), DMEA (N,N-Dimethylethanolamine), DEEA (Diethylethanolamine) and MAPA (N-Methyl-1,3-diaminopropane) are presented. The presented amines are potential solvents for CO_2 post-combustion capture, and they were previously studied for this purposed be several authors (Austgen et al., 1991; Fernandes et al., 2012; Liebenthal et al., 2013; Monteiro et al., 2013a; Monteiro et al., 2013b; Naami et al., 2013; Pinto et al., 2013; Voice et al., 2013). Density data for solutions without absorbed CO_2 (unloaded solutions) are given for the entire composition range for aqueous solutions of all four amines while data for loaded solutions (with absorbed CO_2) are presented for MDEA, DEEA and MAPA. The density of unloaded solutions is modelled by using the Redlich-Kister model with 3 parameters. Since each parameter has a linear temperature dependency, a total 6 parameters were fitted. Literature data, when available, were compared to the experimental data presented in this work and used to validate the regressed models.

This work presents an empirical proportionality model that correlates the density change due to CO_2 loading to the amount of CO_2 loaded. The proposed model is able to adequately predict the density of loaded solutions with only two extra parameters. Models for both unloaded and loaded monoethanolamine (MEA) solutions are also given, regressed using data available in literature, since MEA is the benchmark amine for CO_2 capture (Aroonwilas and Veawab, 2009; Rey et al., 2013) and it's still studied (e.g. see, for instance, Giuffrida et al. (2013), Razi et al. (2013) and Vevelstad et al. (2013)). Finally, a comparison between the performance of the Redlich-Kister and the Rackett models (Rackett, 1970) is presented.

2. Literature data

An overview of experimental density data available in the literature for aqueous solutions of MEA, MDEA, DMEA and DEEA and considered in this work, is presented in Table 1. For MAPA, no prior published density data were found.

TABLE 1 HERE

Table 1: Literature data for unloaded and loaded solutions of MDEA, DMEA, DEEA and MEA considered in this work.

3. Experimental work

3.1 Chemicals

MDEA (N-Methyldiethanolamine), DMEA (N,N-Dimethylethanolamine), DEEA (Diethylethanolamine) and MAPA (N-Methyl-1,3-diaminopropane) were supplied by Sigma-Aldrich and used without further purification. Identification and purity of the used chemicals are given in Table 2. The solutions were prepared by weighing amine and DI water. The loaded solutions were prepared using carbon dioxide (CO_2) with a purity of 99.999% from YaraPraxair.

TABLE 2 HERE

Table 2: Amines studied in this work.

3.2 Preparation and analyses of loaded solutions

Aqueous amine solutions were prepared by weighing and mixing amine and DI water. The CO_2 loaded aqueous solutions of MDEA, DEEA and MAPA were prepared by bubbling CO_2 through unloaded solutions.

The barium chloride method was used to analyse the CO_2 content in solution (mole CO_2/kg solution), while the amine concentration was analysed using titration (Monteiro et al., 2013b). From these analyses the loading was calculated. To ensure that the no amine/water loss was encountered during the loading process, and that the solutions were prepared correctly, the difference between the titrated amine concentration and concentration based on weighing were compared using equation 1, where Δ, C_u^w and $C_u^{tit.}$ are, respectively, the difference, the unloaded amine concentration weighed in (mole amine/kg solution) and the unloaded amine concentration analysed by titration (mole amine/kg solution).

$$\Delta = \frac{C_u^w - C_u^{tit.}}{C_u^w} \qquad 1$$

In case of loaded solutions the amine concentration was back-calculated to unloaded solution according to equation 2 where $C_u^{tit.}$, $C_l^{tit.}$ and $m_{CO_2}^{tit.}$ are the amine concentration in the unloaded solution (mole amine/kg solution), the amine concentration in the loaded solution (mole amine/kg solution) and the concentration of CO_2 in the loaded solution (g CO_2/kg solution), respectively.

$$C_u^{tit.} = \frac{C_l^{tit.}}{\left(\frac{1000\,{}^{g_{l\,sol}}/_{kg_{sol}} - m_{CO_2}^{tit.}}{1000\,{}^{g}/_{kg}} \right)} \qquad 2$$

The difference between the amine concentration calculated based on weighing and amine analyses was 1.3% in average for both loaded and unloaded solutions. This indicated that there was little solvent loss during the loading procedure. The CO_2 analyses were always performed twice and the average difference between the parallels was 1.1 %.

In the next chapter the given amine concentrations are all based on the weighed amounts of amine and water, while the loadings are based on wet chemistry analyses.

3.3 Density measurements

The densities of the solutions were measured by an Anton Paar DMA 4500M densitometer with measuring range from 0 to 3 g /cm^3 and a nominal repeatability of 0.01 kg/m^3 and 0.01^{o}C. A sample of 10 ml was placed in a test tube, and put into the heating magazine with a cap on. The temperature in the magazine was controlled by a Xsampler 452 H heating attachment.

Two density measurements for each sample were done. Two cleaning liquids were used between the samples. Cleaning liquid one was distilled water to remove sample residues in the measuring cell. Cleaning liquid two was acetone to remove cleaning liquid one, and it was evaporated by a stream of dry air in order to accelerate drying of the cell. Both at the beginning and at the end of each day, the density of water was measured and compared with literature values (Wagner and Pruß, 2002). The difference between these measurements was, on average, 0.033 kg/m^3. This value is 3.3 times the given nominal repeatability, and gives an estimate of the measurement uncertainty.

4 Modelling

Several models for calculating densities can be found in the literature. These models either give explicit values for the physical property itself, or values for an excess property which subsequently allows for the physical property calculation. The choice of which correlation to be used is a matter of accuracy and user's choice. In this work the densities of the binary systems were modelled using both an excess volume approach, calculated by a Redlich-Kister type model, and the Rackett model.

4.1 The Redlich-Kister equation

The Redlich-Kister equation, shown in equation 3, is a semi-empirical correlation used to calculate excess properties of solutions as a function of their composition. It was originally proposed to correlate Scatchard's excess free energy (Redlich and Kister, 1948) , but is commonly used for correlating excess volume. It is formulated as a power series of $1-2x_2$, which is a symmetric variable with respect to the two components in a binary solution. The series order will dictate the accuracy of the model predictions; the higher order terms being corrections to the terms of lower order.

The A_n coefficients are optimized parameters and, in this work, have a temperature dependency as given by equation 4.

$$V^E = x_1 x_2 \sum_n A_n \left(1-2x_2\right)^{n-1} \qquad 3$$

$$A_n = a_n + b_n T \qquad 4$$

4.2 Excess volume

The excess molar volume is defined by equation 5. V_{mix}, V_1° and V_2° are the molar volumes of the mixture, pure component 1 and pure component 2, respectively.

$$V^E = V^{mix} - x_1 V_1^\circ - x_2 V_2^\circ \qquad 5$$

The molar volume terms in equation 5 can be written as a function of densities, as given in equation 6. The mixture density is therefore explicitly calculated by rearranging equation 6, where the excess molar volume is given by equation 3.

$$V^E = \left[\frac{x_1 MW_1 + x_2 MW_2}{\rho_{mix}}\right] - x_1 \frac{MW_1}{\rho_1} - x_2 \frac{MW_2}{\rho_2} \qquad 6$$

4.3 The Rackett equation

The Rackett model is an equation of state formulated for saturated liquids. The original model correlates the reduced volumes to the reduced temperature and the critical compressibility factor (Rackett, 1970). This information is readily available in process simulation tools containing the desired components in their databases. Hence, even if no density measurement is available, the Rackett model can be used. Versions of the Rackett model are available in process simulators such as Aspen Plus, Aspen HYSYS, ProII and UniSim Design.

When density data for pure components are available, the Rackett compressibility factor (Z^{RA}) can be regressed in order to minimize the errors in the model's predictions. This value is available in process simulator databases for a number of substances.

There are many modifications of the original Rackett equation in the literature. For instance, the Campbell-Thodos model (Campbell and Thodos, 1984) introduces a temperature dependency to Z^{RA}. On the other hand, many of these modifications introduce extra parameters to the equation, which are not easily found in literature.

In this work, the modified Rackett equation proposed by Spencer and Danner (1972) was used, applying the mixing rules described in equations 7 to 12. These are the same as used in the Aspen Plus process simulator (Aspen Technology, 2012). The density data for pure components was used to regress Z^{RA} for the five amines studied in this work: MEA, MDEA, DMEA, DEEA and MAPA. The critical properties values used in the calculations were obtained from Yaws and Narasimhan (2009). The binary interaction parameter, k_{ij}, was both calculated using equation 13 and treated as an adjustable parameter. By optimizing the parameter the Rackett model was able to better represent the experimental data. A comparison of both approaches is given in the results section.

$$V_m = R\left(\frac{T_c}{P_c}\right)_m \left(Z_m^{RA}\right)^{\left[1+\left(1-T_{rm}\right)^{2/7}\right]} \qquad 7$$

$$\left(\frac{T_c}{P_c}\right)_m = \sum_i x_i \frac{T_{ci}}{P_{ci}} \qquad 8$$

$$Z_m^{RA} = \sum_i x_i Z_i^{RA} \qquad 9$$

$$V_{cm} = \sum_i x_i V_{ci} \quad (10)$$

$$T_{cm} = \sum_i \sum_j x_i x_j V_{ci} V_{cj} \sqrt{T_{ci} T_{cj}} \left(1 - k_{ij}\right) \Big/ V_{cm}^2 \quad (11)$$

$$T_{rm} = \frac{T}{T_{cm}} \quad (12)$$

$$k_{ij} = 1 - \frac{8\sqrt{V_{ci} V_{cj}}}{\left(\sqrt[3]{V_{ci}} + \sqrt[3]{V_{cj}}\right)^3} \quad (13)$$

4.4 Proportionality model for loaded solutions

Equations 14-16 show how the loaded solution density is modelled. The model proposes that the unloaded solution density is to be used as a reference value. This value is then corrected by adding a factor proportional to the mass of CO_2 added to the solution. A linear temperature dependency is assumed in the dimensionless proportionality constant, c. Hence, there are only two extra parameters to be regressed against the experimental data, namely, c_1 and c_2. ω_{CO_2} is the mass of CO_2 added (in grams) per cm^3 of unloaded solution. From the mass fraction of the unloaded solution it is possible to calculate the number of moles of amine per gram of unloaded solution $\left(N_{amine}\right)$, and by multiplying this by the loading (mole CO_2/mole amine), the molecular weight of CO_2 (g CO_2/mole CO_2) and the density of the unloaded solution at 298.15 K (g of solution/cm^3 of unloaded solution) the mass of CO_2 added to the solution is calculated. It is important to note that equation **15** does not consider a volume expansion or contraction when the CO_2 is added to the solution. This effect is taken into account by *c* given by equation **16**.

$$\rho_{mix}^{loaded} = \rho_{mix}^{unloaded} + c.\omega_{CO_2} \quad (14)$$

$$\omega_{CO_2} = m_{CO_2}\, \rho_{mix}^{unloaded}\Big|_{298.15K} = \alpha N_{amine} MW_{CO_2}\, \rho_{mix}^{unloaded}\Big|_{298.15K} \quad (15)$$

$$c = c_1 + c_2 T \quad (16)$$

5 Optimization routine

Several optimization procedures are available and well discussed in the literature. Usually, gradient based methods are used to find the best parameters to fit a set of experimental data. Those methods, however, require good initial guesses for the parameters.

Alternatively, in this work, the parameters were found using the particle swarm optimization (PSO) algorithm (Kennedy and Eberhart, 1995), which is an heuristic global optimization method. It has the advantage of not requiring initial guesses. Several variations of the method can be found elsewhere (Clerc and Kennedy, 2002; Trelea, 2003; Wang et al., 2011; Yiqing et al., 2007). One important feature of PSO is the way the particles interact with each other, usually called topology. In this work, the lbest topology with dynamic neighbourhood (Ghosh et al., 2012) is used. A comprehensive description on the PSO method is given in Poli et al. (2007).

The candidate solutions were randomly initialized within the intervals [-10, 10] and [-1e-4, 1e-4] for the parameters a_n and b_n (equation 4), respectively. The objective function (equation 17) presented in Weiland et al. (1993) weigh all the data equally, and was chosen to minimize the deviation between the experimental and the calculated densities.

$$F_{obj} = \sum_{i=1}^{N} \frac{\left(\rho_i^E - \rho_i^C\right)^2}{\rho_i^E \rho_i^C} \qquad 17$$

The average absolute relative deviation (AARD) and the absolute average deviation (AAD), given in equations 18 and 19 respectively, express the deviation of the model.

$$AARD(\%) = \frac{100}{N} \sum_{i=1}^{N} \frac{\left|\rho_i^E - \rho_i^C\right|}{\rho_i^E} \qquad 18$$

$$AAD\left(kg/m^3\right) = \frac{1000}{N} \sum_{i=1}^{N} \left|\rho_i^E - \rho_i^C\right| \qquad 19$$

6 Results and Discussions

In this section the experimental results together with the modelled results are discussed. The tabulated values of measured densities for unloaded and loaded solutions are available in the appendix.

6.1 Density of pure amines

The Redlich-Kister equation correlates the excess volume, calculated from the measured amine-water solution densities, the solution composition, as well as the pure amine and pure water densities. It is therefore convenient to express the densities of the pure components as continuous functions of temperature.

The temperature dependency was modelled as a second order polynomial function, according to equation 20. The parameters regressed for water, MEA, MDEA, DMEA, DEEA and MAPA are given in Table 3, along with the coefficient of determination, denoted R^2, and the data references. The densities are given in g/cm^3 and the temperatures are in K.

$$\rho_{pure}\left(g/cm^3\right) = d_1 T^2\left(K\right) + d_2 T\left(K\right) + d_3 \qquad 20$$

TABLE 3 HERE

Table 3: Coefficients for equation 20 describing the densities of pure solvents and water.

Pure water density data given in Wagner and Pruß (2002) from 280 to 373.124 K at 101.325 kPa were used in this work to model the density of water as function of temperature. Figure 1 shows that a second order polynomial function is able to describe the density temperature dependency of pure water. The pure densities for the amines were also well represented by the second order polynomial function as observed from the values of R^2.

FIGURE 1 HERE

Figure 1: Water density as function of temperature.

The Rackett model was also used for calculating the densities of pure amines. The parameters for this model were regressed using the same data as used for regressing the polynomial expressions, and are given in Table 4. From an engineering point of view, the agreement between the model and the data is reasonable. However, the obtained average deviations are two to three orders of magnitude higher than the expected measurement uncertainties.

TABLE 4 HERE

Table 4: Z^{RA} parameters and the calculated deviation for densities of pure amines.

The Rackett equation performs worse than the second order polynomial equation, but gives a reasonable representation of the densities of the pure substances studied in this work, apart from DEEA.

6.2 Density of unloaded solutions

The regressed parameters for the Redlich-Kister model for the unloaded amine-water systems, and the interaction parameters for the Rackett model are given in Table 5. The calculated deviations are given in **Table 6**. In general, the Redlich-Kister model is one order of magnitude more accurate than the Rackett model. The experimental data are given in Table A.1, Table A.2, Table A.3 and Table A.4, for MDEA, DMEA, DEEA and MAPA, respectively.

TABLE 5 HERE

Table 5: Regressed parameters for the Redlich-Kister (a_n and b_n) and the Rackett ($k_{H_2O\text{-Amine}}$) models for calculation of densities of unloaded amine solutions

6.2.1 MEA

The MEA system was modelled using only data from Han et al. (2012b). There are several other sources of data for the unloaded MEA (e.g. Touhara et al. (1982), Maham et al. (1994) and Pouryousefi and Idem (2008)). However, Han et al. (2012b) presents a wider range of data with respect to temperature, and, therefore, only those data were used in the fitting of the parameters.

The whole range of compositions was used in the fitting. However, only data measured at atmospheric pressure were used (from 298.15 to 363.15 K) because the correlations for pure water and pure MEA are only valid at atmospheric pressure. When calculating the density of pure water using the correlation given in equation 20 and parameters given on **Table 3** (for atmospheric conditions) and comparing it with experimental data from Han et al. (2012b) at 0.7 MPa, the deviation can be as high as 5.8 kg/m^3 (at 423.15 K). This is one order of magnitude higher than the deviations calculated within the validity range (from 280 to 373.124 K at 101.325 kPa). This “inaccuracy” in calculating the pure water density will impact the Redlich-Kister density model especially close to the pure water concentrations. Therefore, a pressure dependency should be included in the pure component correlations in

order to obtain similar accuracy (< 0.5 kg/m^3). In this work, the pressure dependency is not included since only data at atmospheric pressure were generated.

The good agreement between the Redlich-Kister model and the experimental data can be seen in Figure 3. It's also possible to see that the Hawrylak et al. (2000) measurements (circle markers in Figure 3) have a small disagreement with the Han et al.(2012b) data at 45ºC, more pronounced at high amine concentrations. This disagreement is also found at 45 ºC for the densities of other amines solutions reported by Hawrylak et al. (2000)(MDEA, DMEA and DEEA).

The maximum absolute deviation between the regressed Redlich-Kister model and the data from Hawrylak et al. (2000) is the highest found in this work as seen on **Table 6**. However, when studying the deviations between the Rackett model and the data from Hawrylak et al. (2000), the same behaviour is not observed. This might be explained by the higher inaccuracy of the Rackett model compared with the Redlich-Kister model. Nevertheless, the deviation of Rackett model is still acceptable for engineering purposes. A comparison between the Redlich-Kister type of model and the Rackett model for the densities of unloaded MEA solutions at 298.15 K is shown in Figure 2.

FIGURE 2 HERE

Figure 2: Densities for MEA aqueous solution at 298.15 K: (▬) Redlich-Kister model, (- -) Rackett model and data from (o) Han et al. (2012b)

It's important to note that when using 3 Redlich-Kister parameters, the deviations presented a systematic trend. This trend is eliminated when using 4 Redlich-Kister parameters as shown in Figure 4, and the fit becomes better. For the model with 4 Redlich-Kister parameters, the AARD and the maximum absolute deviation are 0.014% and 0.57 kg/m^3, respectively. The improvement is significant when adding one more Redlich-Kister parameter. However, the accuracy with 3 Redlich-Kister parameters is still good enough for engineering purposes and is comparable with what is reported in Han et al. (2012b). Therefore, 3 Redlich-Kister parameters were chosen for modelling the systems studied although a trend is presented in the deviations for all systems.

FIGURE 3 HERE

Figure 3:. Density for unloaded MEA-water system. Experimental data: (o) from Hawrylak et al. (2000), (Δ) from Han et al. (2012b), (□) from Amundsen et al. (2009), (*) from Touhara et al. (1982) and (□) from Kapadi et al. (2002). Temperatures: 298.15 K (Red), 303.15 K (Green), 308.15 K (Orange), 313.15 K (Blue), 318.15 K (Yellow), 323.15 K (Dark Pink),

328.15 K (Brown), 333.15 K (Violet), 338.15 K (Light Green), 343.15 K (Dark Brown), 348.15 K (Pink), 353.15 K (Light Brown), 358.15 K (Light Blue), 363.15 K (Beige).

FIGURE 4 HERE

Figure 4: Deviations on density for MEA-water system. (o) Experimental data from Han et al. (2012b). (A) fit with: (A) 3 Redlich-Kister parameters, (B) 4 Redlich-Kister parameters.

6.2.2 MDEA

The density for the unloaded MDEA-water system was modelled using experimental data from this work for the whole range of compositions and from 293.15 to 353.15 K. The deviations between the regressed models and the experimental values are given in Table 6. There is good agreement between the regressed models and the experimental data. The ratio between the Redlich-Kister model results and the experimental data can be seen in Figure 5.

Han et al. (2012a) also present data for the water-MDEA system measured at 363.15 K, but these were not used in the Redlich-Kister parameter optimization. Even if the highest temperature used for model regression was 353.15K, the model is able to predict the density at 363.15 K with a maximum deviation of 1.44 kg/m^3. This value is satisfactory since the maximum absolute deviation between the model and the experiments from Han et al. (2012a) was 1.95 kg/m^3 at 303.15 K.

FIGURE 5 HERE

Figure 5: Ratio between calculated and experimental data for MDEA-water unloaded system. Experimental data: (o) from Maham et al. (1995), (Δ) from Hawrylak et al. (2000), (□) from Han et al. (2012a), (*) from Chowdhury et al. (2009), and (★) This Work.

6.2.3 DMEA

Again, only data produced in this work were used for modelling the density of unloaded aqueous solutions of DMEA. Figure 6 shows the ratio between calculated densities using the Redlich-Kister model and the experimental data. The maximum calculated deviation was 2.15 kg/m^3 using the Redlich-Kister model, and 21.36 kg/m^3 using the Rackett model. In Table 6, the deviations for all sources are reported.

FIGURE 6 HERE

Figure 6: Ratio between calculated and experimental data for DMEA-water unloaded system. (**o**) experimental data from Zhang et al. (1995), (Δ) experimental data Hawrylak et al. (2000), (□) experimental data from This Work.

6.2.4 DEEA

The density of the DEEA-water system was also estimated using only data presented in this work. The models were able to represent well the experimental data. The maximum absolute deviation for the data used in the optimization was 1.54 kg/m^3 for the Redlich-Kister model and 23.61 kg/m^3 for the Rackett model. Two other literature sources were used to validate the model and the deviations are reported on Table 6. Figure 7 shows the ratio between the calculated densities using the Redlich-Kister model and the experimental data for the three sources.

FIGURE 7 HERE

Figure 7: Ratio between calculated and experimental data for DEEA-water unloaded system. (**o**) experimental data from Zhang et al. (1995), (Δ) experimental data Hawrylak et al. (2000), (□) experimental data from this work.

6.2.5 MAPA

No density data for MAPA were found to be available in the literature. The density for the unloaded system of MAPA-water system was estimated using only data presented in this work for the whole range of compositions and from 298.15 to 353.15 K. The deviations are given in Table 6 for both models. The Redlich-Kister model and the experimental data are shown in Figure 8. The highest deviations occurred for 0.2 and 0.3 mole fraction of MAPA.

FIGURE 8 HERE

Figure 8: (A) Density for unloaded MAPA-water system. Experimental data: (**o**) from This Work. Temperatures: 298.15 K (Red), 303.15 K (Green), 313.15 K (Orange), 323.15 K (Blue), 333.15 K (Yellow), 343.15 K (Dark Pink), 353.15 K (Brown). (B) Ratio between calculated and experimental data for MAPA-water unloaded system.

TABLE 6 HERE

Table 6: Calculated deviations for the unloaded amine-water systems

6.3 Density of loaded Solutions

Densities of loaded solutions were also measured and modelled in this work. Table 7 shows the parameters of the models presented in this work while the calculated deviations are presented in Table 8.

The densities of the unloaded solutions were required to calculate the density of the loaded solutions using the proportionality model. Assuming the linear temperature dependency suggested by equation 16, the density of the loaded solutions could be modelled with only two extra parameters giving a total of 8 parameters. In comparison Han et al. (2012b) modelled the density of loaded MEA solutions using 17 parameters.

When using the Rackett model, binary interaction parameters are needed. Because no data for carbonated water solutions were used, equation 13 was used to compute the value of $k_{\mathrm{H_2O\text{-}CO_2}}$, which was found as 0.01114. The only extra parameter to be regressed is then $k_{\mathrm{CO_2\text{-}Amine}}$. The experimental measurements are given in the appendix in Tables A.5, A.6 and A.7 for MDEA, DEEA and MAPA, respectively,

6.3.1 MEA

No data for loaded MEA solutions was generated in this work. Instead, data from Han et al. (2012b) measured at atmospheric pressure were used for modelling this system. The proportionality model was able to calculate the densities of the loaded MEA solutions with satisfactory accuracy. The deviations are comparable to what is reported in Han et al. (2012b). Figure 9 shows the deviations calculated with the optimized proportionality model.

FIGURE 9 HERE

Figure 9: Ratio between the calculated and experimental densities for MEA loaded solutions. Proportionality model optimized using only data form Han et al. (2012b)..

6.3.2 MDEA

For the loaded MDEA system, two approaches were used to calculate the densities. First, only data generated in this work were used and the models were later compared to literature data. In this work densities for loaded 2 M (~23.8% mass) and 4.2 M (~50% mass) MDEA solutions were measured. The proportionality model was able to accurately predict the experimental data with a maximum absolute deviation of 3.4 kg/m^3, whereas the Rackett

model gives a maximum deviation of 25.1 kg/m^3. Experimental data from Han et al. (2012a) were also well predicted by the proportionality model. The deviations are within 1%, as can be observed in Figure 10.

Data from Weiland et al. (1998) up to 50 % mass MDEA are also reasonably predicted by the proportionality model. Nonetheless, for the 60% mass MDEA solution, high deviations between the proportionality model and experimental data are seen. Neither the proportionality model nor the Rackett model are able to accurately predict the density of the 60% mass MDEA solution, and the maximum deviations are 44.4 and 45.1 kg/m^3, for the two regressed models, respectively.

In the second approach we used the combined data from Weiland et al. (1998), Han et al. (2012a) and this work for regression. This model compromises the accuracy in representing the data in this work in order to improve the accuracy with respect to the two other sources. This behaviour was expected since the two other sources comprise larger amounts of data, and hence, will have a greater impact in the objective function minimization. However, still the data series for 60 mass% MDEA from Weiland et al. (1998) show large deviations in both models. Figure 11 shows the ratio between the calculated densities using the proportionality model and experimental data.

FIGURE 10 HERE

Figure 10: Ratio between the calculated and experimental densities for MDEA loaded solutions. Proportionality model optimized using only data form this work.

FIGURE 11 HERE

Figure 11: Ratio between the calculated and experimental densities for MDEA loaded solutions. Model optimized using all data from Weiland et al. (1998), Han et al. (2012a) and this work.

6.3.3 DEEA

No density data for loaded DEEA solutions were found in the literature. Density measurements were performed in loaded DEEA aqueous solutions with 24 and 61mass % DEEA from 293.15 to 343.15 K. The density seems to have a linear dependency on loading. The experiments done for the 24 mass% DEEA, at loadings around 0.4, appear to be slightly shifted. The reason might be a small uncertainty in the density measurements or in the calculation of the loading. FIGURE 12 HERE

Figure **12** shows the experimental data and the calculated densities using the proportionality model for the loaded DEEA solutions. The maximum absolute deviation is calculated to be 11.5 kg/m^3 for the proportionality model and 34.0 kg/m^3 for the Rackett model.

FIGURE 12 HERE

Figure 12: Calculated densities using the proportionality model for: (A) DEEA 24% mass and (B) DEEA 61% mass. Experimental data: (★) from This Work. Temperatures: 293.15 K (Red), 303.15 (Green), 313.15 K (Orange), 323.15 K (Blue), 333.15 K (Yellow), 343.15 K (Dark Pink).

6.3.4 MAPA

No density data for loaded MAPA solutions were found in the literature. The density for 18 and 46 mass % MAPA solutions loaded with CO_2 was measured from 293.15 to 323.15 K. Figure 13 shows the comparison between the experimental data and the proportionality model. As for the DEEA measurements, the data for the 18 mass% solution at loading around 0.5 seem to be slightly off. Two measurements for the 46% solution at higher loadings were not included in the optimization, yet they are given together with the other data in Table A.7.

The proportionality model predicts the density of loaded solutions of MAPA reasonably well with a maximum absolute deviation of 6.3 kg/m^3, whereas the maximum absolute deviation when using the Rackett model is 34.0 kg/m^3.

FIGURE 13 HERE

Figure 13: Calculated densities using the proportionality model for: (A) MAPA 18% mass and (B) MAPA 46% mass. Experimental data: (★) from This Work. Temperatures: 293.15 K (Red), 303.15 (Green), 313.15 K (Orange), 323.15 K (Blue).

TABLE 7 HERE

Table 7: Parameters for loaded systems.

TABLE 8 HERE

Table 8: Deviations for loaded systems.

7 Conclusions

New density data for aqueous unloaded and loaded amine solutions were generated in this work. The density measurements were compared to literature data whenever they existed. Excellent agreement with literature data was observed, especially for unloaded systems. The deviations between density measurements from different sources are smaller for unloaded solutions than for the loaded solutions. This is due to more sources of error present when loaded experiments are performed, e.g. CO_2 loading determinations and the possibility of CO_2 stripping off during the experiments.

A Redlich-Kister model with a linear temperature dependency in the Redlich-Kister parameters was proposed for modelling the density of unloaded solutions. The model was able to accurately predict the experimental data with a total of 3 parameters. An increase to 4 parameters led to a significant improvement in accuracy, but taking into account the good predictions with only 3 parameters and the added model complexity from adding an extra parameter, it was concluded that 3 parameters were sufficient for modelling densities of unloaded solutions.

The Rackett model was also tested in this work. It is shown that the Rackett model can be used to give reasonable estimates for the liquid densities. However, the accuracy is in general one order of magnitude lower than for the Redlich-Kister fit. Fitting the binary interaction coefficient in the Racket model (mixing rule) did not give a significant improvement in the accuracy.

For loaded solution densities, a simple proportionality model was proposed. Thereby the density of loaded solutions could be modelled using the unloaded solutions density models and only two extra parameters. This model satisfactorily predicts the densities of loaded solutions, and the results are significantly better than with the Rackett model (the maximum absolute deviation calculated with the proportionality model could be 8 times smaller than the deviation calculated with the Rackett model).

The densities of four possible solvents for CO_2 capture were measured over a wide range of temperatures and compositions, and for both loaded and unloaded solutions. These densities, together with literature data for MEA solutions, were well correlated by the developed models, making them suitable for use in process simulators to better predict and simulate CO_2 capture process. This work thus provides density correlations for a total of five possible solvents for CO_2 capture.

Acknowledgments

Financial support from the EC 7th Framework Programme through Grant Agreement No : iCap-241391, is gratefully acknowledged. The authors would also like to acknowledge the experimental work carried out by Brice Pinteaux and Morgane Séné.

Appendix A: Density data for unloaded solutions

TABLE A.1 HERE

Table A.1: Density for the unloaded aqueous MDEA solutions at different temperatures.

TABLE A.2 HERE

Table A.2: Density for the unloaded aqueous DMEA solutions at different temperatures.

TABLE A.3 HERE

Table A.3: Density for the unloaded aqueous DEEA solutions at different temperatures.

TABLE A.4 HERE

Table A.4: Density for the unloaded aqueous MAPA solutions at different temperatures.

TABLE A.5 HERE

Table A.5: Density of loaded solutions of aqueous MDEA solutions at different temperatures.

TABLE A.6 HERE

Table A.6: Density of loaded solutions of aqueous DEEA solutions at different temperatures.

TABLE A.7 HERE

Table A.7: Density of loaded solutions of aqueous MAPA solutions at different temperatures.

References

Aroonwilas, A., Veawab, A., 2009. Integration of CO_2 capture unit using blended MEA–AMP solution into coal-fired power plants. Energy Procedia 1, 4315-4321.

Aspen Technology, I., 2012. Aspen Physical Property System - Physical Property Models. Version Number: V7.3.2.

Austgen, D.M., Rochelle, G.T., Chen, C.C., 1991. Model of vapor-liquid equilibria for aqueous acid gas-alkanolamine systems. 2. Representation of hydrogen sulfide and carbon dioxide solubility in

598 aqueous MDEA and carbon dioxide solubility in aqueous mixtures of MDEA with MEA or DEA.
599 Industrial & Engineering Chemistry Research 30, 543-555.

600 Campbell, S.W., Thodos, G., 1984. Saturated liquid densities of polar and nonpolar pure substances.
601 Industrial & Engineering Chemistry Fundamentals 23, 500-510.

602 Cheng, S., Meisen, A., Chakma, A., 1996. Predict amine solution properties accurately. Hydrocarbon
603 Processing 75, 81-84.

604 Clerc, M., Kennedy, J., 2002. The particle swarm - explosion, stability, and convergence in a
605 multidimensional complex space. Evolutionary Computation, IEEE Transactions on 6, 58-73.

606 Fernandes, D., Conway, W., Wang, X., Burns, R., Lawrance, G., Maeder, M., Puxty, G., 2012.
607 Protonation constants and thermodynamic properties of amines for post combustion capture of CO_2.
608 The Journal of Chemical Thermodynamics 51, 97-102.

609 Ghosh, S., Das, S., Kundu, D., Suresh, K., Abraham, A., 2012. Inter-particle communication and
610 search-dynamics of lbest particle swarm optimizers: An analysis. Information Sciences 182, 156-168.

611 Giuffrida, A., Bonalumi, D., Lozza, G., 2013. Amine-based post-combustion CO_2 capture in air-blown
612 IGCC systems with cold and hot gas clean-up. Applied Energy 110, 44-54.

613 Han, J., Jin, J., Eimer, D.A., Melaaen, M.C., 2012a. Density of Water (1) + Diethanolamine (2) + CO2
614 (3) and Water (1) + N-Methyldiethanolamine (2) + CO2 (3) from (298.15 to 423.15) K. Journal of
615 Chemical & Engineering Data 57, 1843-1850.

616 Han, J., Jin, J., Eimer, D.A., Melaaen, M.C., 2012b. Density of Water (1) + Monoethanolamine (2) +
617 CO2 (3) from (298.15 to 413.15) K and Surface Tension of Water (1) + Monoethanolamine (2) from
618 (303.15 to 333.15) K. Journal of Chemical & Engineering Data 57, 1095-1103.

619 Hartono, A., Svendsen, H.F., 2009. Density, viscosity, and excess properties of aqueous solution of
620 diethylenetriamine (DETA). The Journal of Chemical Thermodynamics 41, 973-979.

621 Hawrylak, B., Burke, S., Palepu, R., 2000. Partial Molar and Excess Volumes and Adiabatic
622 Compressibilities of Binary Mixtures of Ethanolamines with Water. Journal of Solution Chemistry 29,
623 575-594.

624 Kennedy, J., Eberhart, R., 1995. Particle swarm optimization, Neural Networks, 1995. Proceedings.,
625 IEEE International Conference on, pp. 1942-1948 vol.1944.

626 Liebenthal, U., Pinto, D.D.D., Monteiro, J.G.M.S., Svendsen, H.F., Kather, A., 2013. Overall Process
627 Analysis and Optimisation for CO2 Capture from Coal Fired Power Plants based on Phase Change
628 Solvents Forming Two Liquid Phases. Energy Procedia 37, 1844-1854.

Maham, Y., Teng, T., Hepler, L., Mather, A., 1994. Densities, excess molar volumes, and partial molar volumes for binary mixtures of water with monoethanolamine, diethanolamine, and triethanolamine from 25 to 80°C. Journal of Solution Chemistry 23, 195-205.

Mokraoui, S., Valtz, A., Coquelet, C., Richon, D., 2006. Volumetric properties of the isopropanolamine–water mixture at atmospheric pressure from 283.15 to 353.15K. Thermochimica Acta 440, 122-128.

Monteiro, J.G.M.S., Pinto, D.D.D., Luo, X., Knuutila, H., Hussain, S., Mba, E., Hartono, A., Svendsen, H.F., 2013a. Activity-based Kinetics of the Reaction of Carbon Dioxide with Aqueous Amine Systems. Case Studies: MAPA and MEA. Energy Procedia 37, 1888-1896.

Monteiro, J.G.M.S., Pinto, D.D.D., Zaidy, S.A.H., Hartono, A., Svendsen, H.F., 2013b. VLE data and modelling of aqueous N,N-diethylethanolamine (DEEA) solutions. International Journal of Greenhouse Gas Control 19, 432-440.

Naami, A., Sema, T., Edali, M., Liang, Z., Idem, R., Tontiwachwuthikul, P., 2013. Analysis and predictive correlation of mass transfer coefficient of blended MDEA-MEA for use in post-combustion CO_2 capture. International Journal of Greenhouse Gas Control 19, 3-12.

Pinto, D.D.D., Monteiro, J.G.M.S., Bersås, A., Haug-Warberg, T., Svendsen, H.F., 2013. eNRTL Parameter Fitting Procedure for Blended Amine Systems: MDEA-PZ Case Study. Energy Procedia 37, 1613-1620.

Poli, R., Kennedy, J., Blackwell, T., 2007. Particle swarm optimization. Swarm Intelligence 1, 33-57.

Pouryousefi, F., Idem, R.O., 2008. New Analytical Technique for Carbon Dioxide Absorption Solvents. Industrial & Engineering Chemistry Research 47, 1268-1276.

Rackett, H.G., 1970. Equation of state for saturated liquids. Journal of Chemical & Engineering Data 15, 514-517.

Razi, N., Svendsen, H.F., Bolland, O., 2013. Cost and energy sensitivity analysis of absorber design in CO_2 capture with MEA. International Journal of Greenhouse Gas Control 19, 331-339.

Redlich, O., Kister, A.T., 1948. Algebraic Representation of Thermodynamic Properties and the Classification of Solutions. Industrial & Engineering Chemistry 40, 345-348.

Rey, A., Gouedard, C., Ledirac, N., Cohen, M., Dugay, J., Vial, J., Pichon, V., Bertomeu, L., Picq, D., Bontemps, D., Chopin, F., Carrette, P.L., 2013. Amine degradation in CO_2 capture. 2. New degradation products of MEA. Pyrazine and alkylpyrazines: Analysis, mechanism of formation and toxicity. International Journal of Greenhouse Gas Control 19, 576-583.

660 Spencer, C.F., Danner, R.P., 1972. Improved equation for prediction of saturated liquid density.
661 Journal of Chemical & Engineering Data 17, 236-241.

662 Touhara, H., Okazaki, S., Okino, F., Tanaka, H., Ikari, K., Nakanishi, K., 1982. Thermodynamic
663 properties of aqueous mixtures of hydrophilic compounds 2. Aminoethanol and its methyl
664 derivatives. The Journal of Chemical Thermodynamics 14, 145-156.

665 Trelea, I.C., 2003. The particle swarm optimization algorithm: convergence analysis and parameter
666 selection. Information Processing Letters 85, 317-325.

667 Vevelstad, S.J., Grimstvedt, A., Elnan, J., da Silva, E.F., Svendsen, H.F., 2013. Oxidative degradation of
668 2-ethanolamine: The effect of oxygen concentration and temperature on product formation.
669 International Journal of Greenhouse Gas Control 18, 88-100.

670 Voice, A.K., Vevelstad, S.J., Chen, X., Nguyen, T., Rochelle, G.T., 2013. Aqueous 3-
671 (methylamino)propylamine for CO_2 capture. International Journal of Greenhouse Gas Control 15, 70-
672 77.

673 Wagner, W., Pruß, A., 2002. The IAPWS Formulation 1995 for the Thermodynamic Properties of
674 Ordinary Water Substance for General and Scientific Use. Journal of Physical and Chemical Reference
675 Data 31, 387-535.

676 Wang, Y., Li, B., Weise, T., Wang, J., Yuan, B., Tian, Q., 2011. Self-adaptive learning based particle
677 swarm optimization. Information Sciences 181, 4515-4538.

678 Weiland, R.H., Chakravarty, T., Mather, A.E., 1993. Solubility of carbon dioxide and hydrogen sulfide
679 in aqueous alkanolamines. Industrial & Engineering Chemistry Research 32, 1419-1430.

680 Weiland, R.H., Dingman, J.C., Cronin, D.B., Browning, G.J., 1998. Density and Viscosity of Some
681 Partially Carbonated Aqueous Alkanolamine Solutions and Their Blends. Journal of Chemical &
682 Engineering Data 43, 378-382.

683 Yaws, C.L., Narasimhan, P.K., 2009. Chapter 1 - Critical properties and acentric factor—Organic
684 compounds, in: Carl, L.Y. (Ed.), Thermophysical Properties of Chemicals and Hydrocarbons. William
685 Andrew Publishing, Norwich, NY, pp. 1-95.

686 Yiqing, L., Xigang, Y., Yongjian, L., 2007. An improved PSO algorithm for solving non-convex
687 NLP/MINLP problems with equality constraints. Computers & Chemical Engineering 31, 153-162.

688 Zhang, F.-Q., Li, H.-P., Dai, M., Zhao, J.-P., Chao, J.P., 1995. Volumetric properties of binary mixtures
689 of water with ethanolamine alkyl derivatives. Thermochimica Acta 254, 347-357.

690

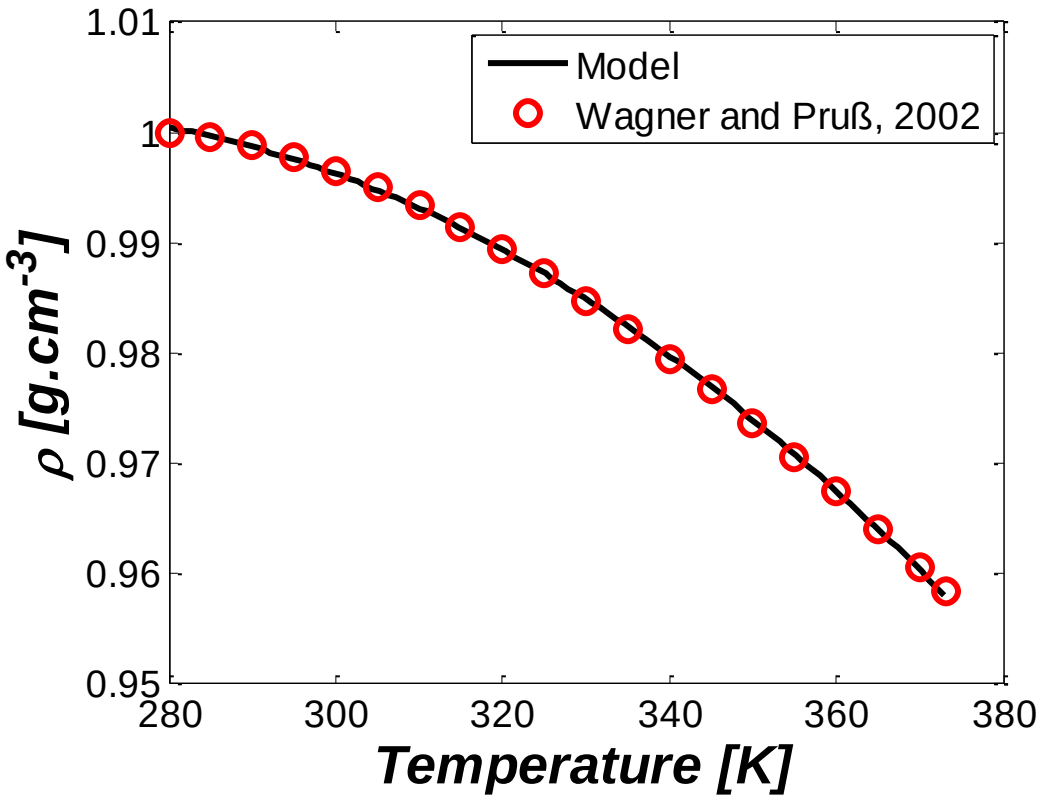

Figure 1: Water density as function of temperature.

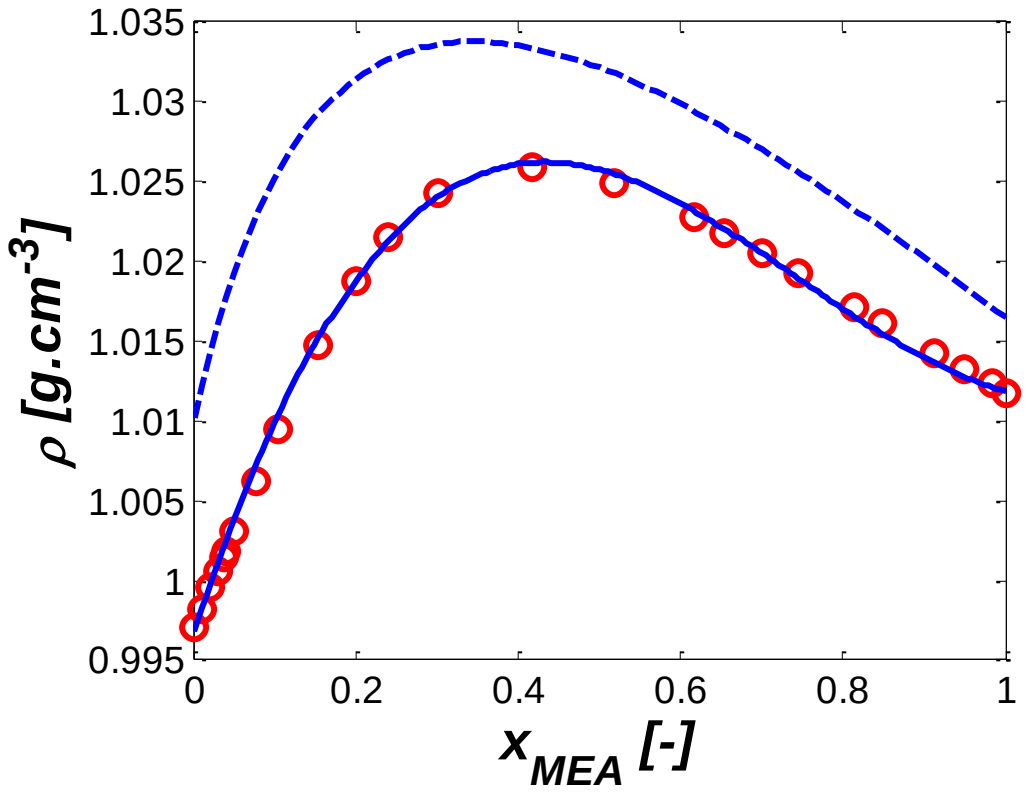

Figure 2: Densities for MEA aqueous solution at 298.15 K: (—) Redlich-Kister model, (- -) Rackett model and data from (o) Han et al. (2012b).

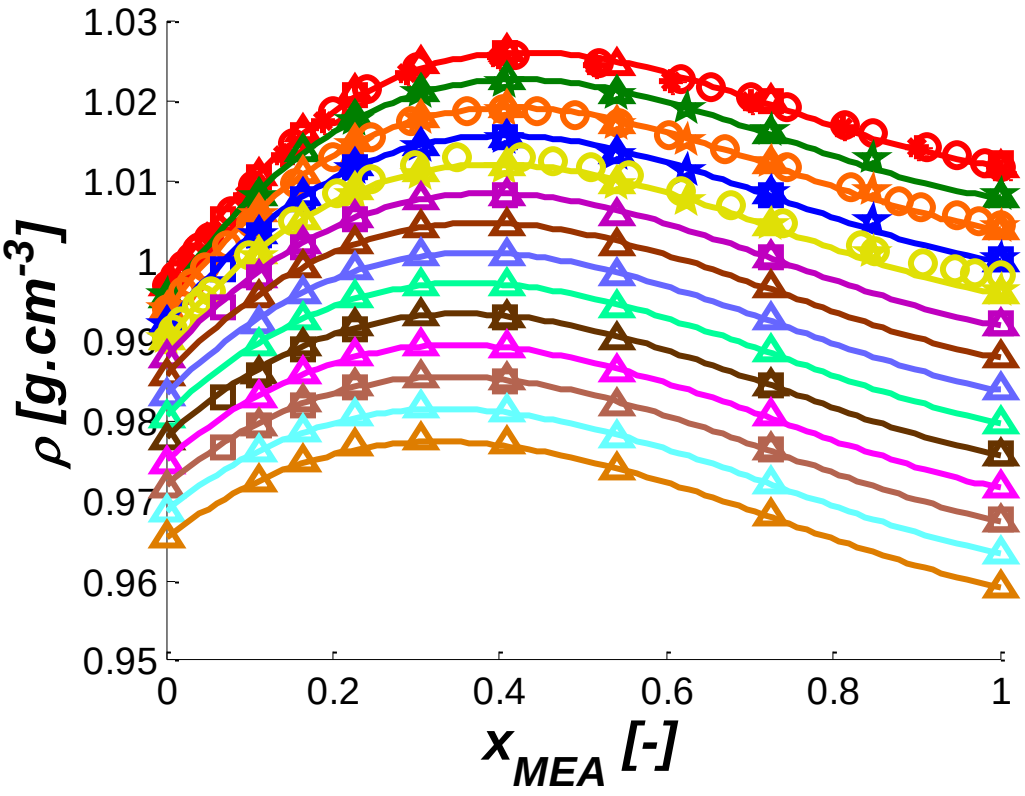

Figure 3: Density for unloaded MEA-water system. Experimental data: (**o**) from Hawrylak et al. (2000), (Δ) from Han et al. (2012b), (□) from Amundsen et al. (2009), (*) from Touhara et al. (1982) and (★) from Kapadi et al. (2002). Temperatures: 298.15 K (Red), 303.15 K (Green), 308.15 K (Orange), 313.15 K (Blue), 318.15 K (Yellow), 323.15 K (Dark Pink), 328.15 K (Brown), 333.15 K (Violet), 338.15 K (Light Green), 343.15 K (Dark Brown), 348.15 K (Pink), 353.15 K (Light Brown), 358.15 K (Light Blue), 363.15 K (Beige).

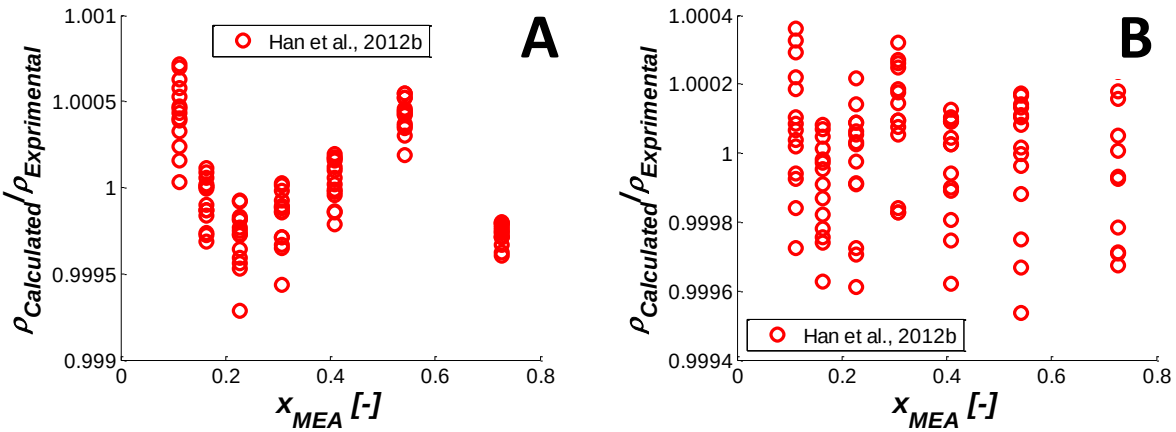

Figure 4: Deviations on density for MEA-water system. (o) Experimental data from Han et al. (2012b). (A) fit with: (A) 3 Redlich-Kister parameters, (B) 4 Redlich-Kister parameters.

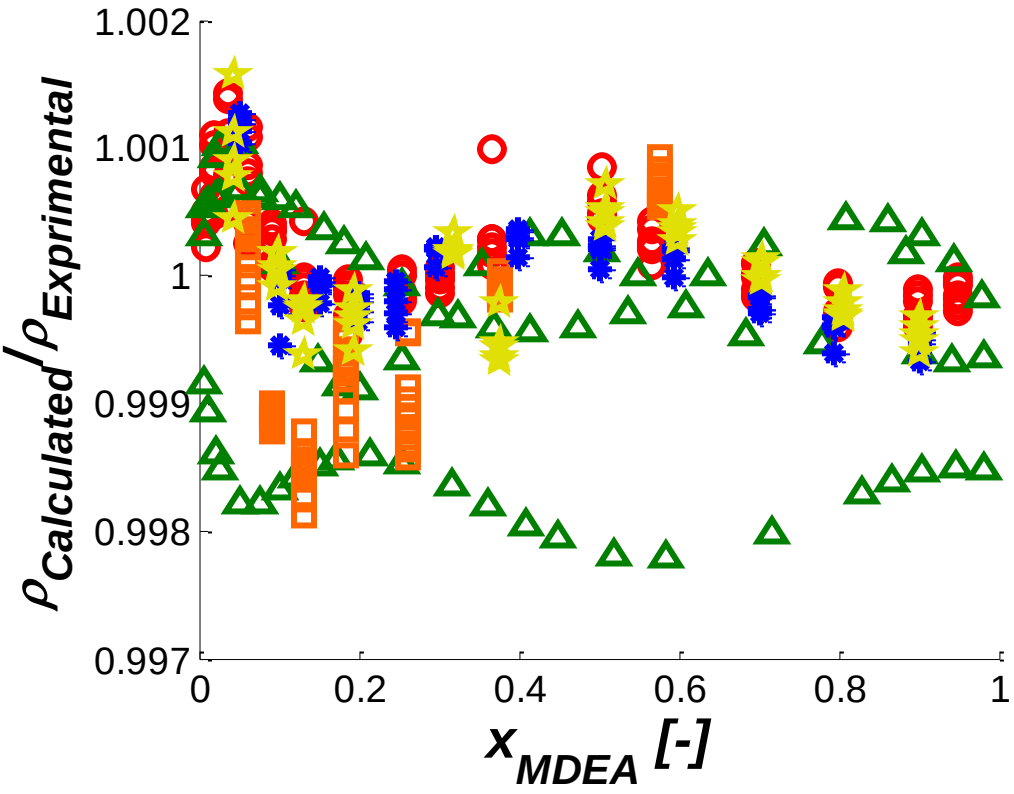

Figure 5: Ratio between calculated and experimental data for MDEA-water unloaded system. Experimental data: (o) from Maham et al. (1995), (Δ) from Hawrylak et al. (2000), (□) from Han et al. (2012a), (*) from Chowdhury et al. (2009), and (★) This Work.

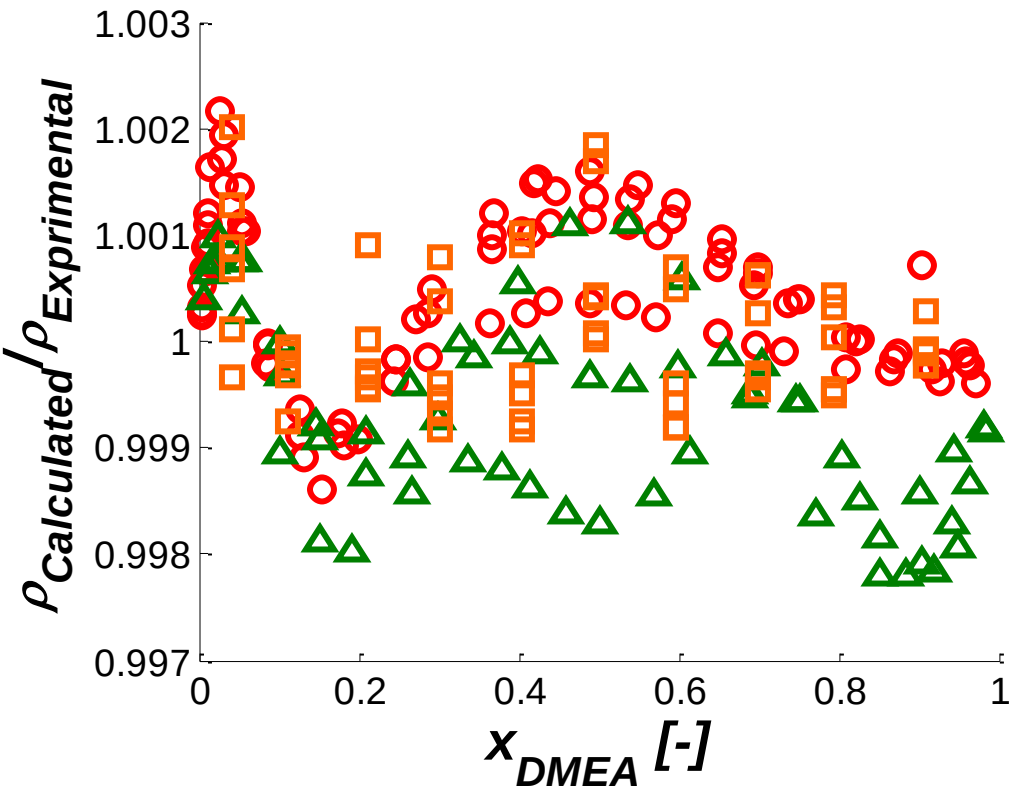

Figure 6: Ratio between calculated and experimental data for DMEA-water unloaded system. Experimental data: (**o**) experimental data from Zhang et al. (1995), (Δ) experimental data Hawrylak et al. (2000), (□) experimental data from This Work.

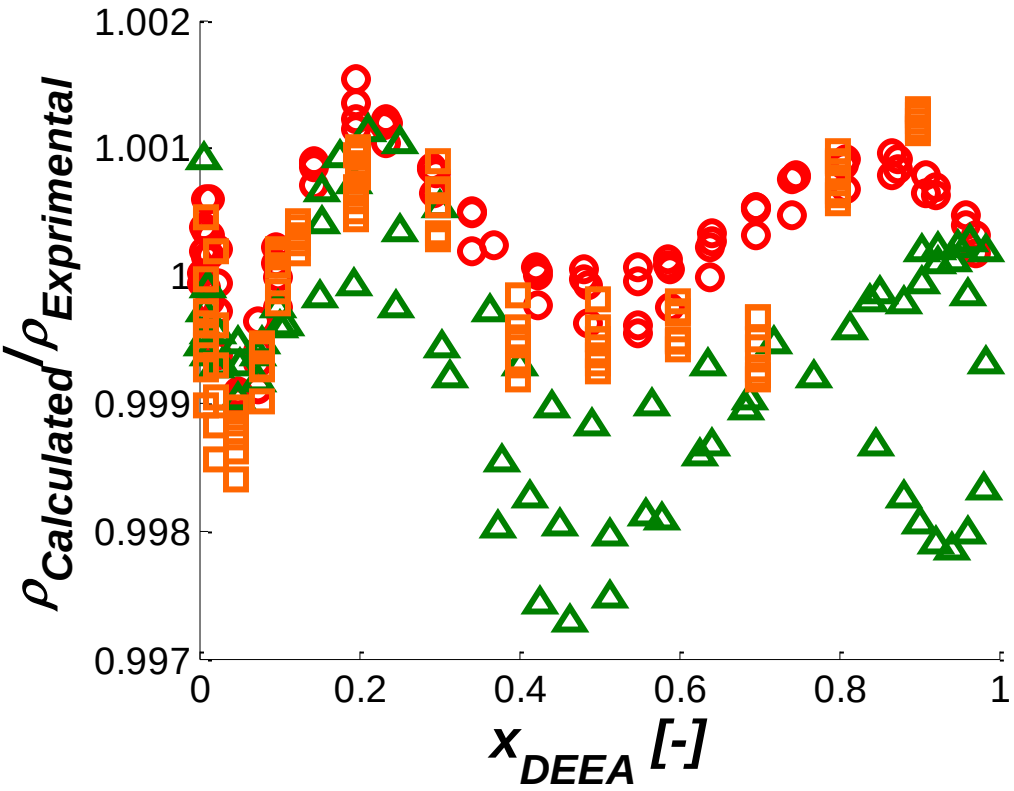

Figure 7: Ratio between calculated and experimental data for DEEA-water unloaded system. Experimental data: (**o**) from Zhang et al. (1995), (Δ) from Hawrylak et al. (2000), (□) from This Work.

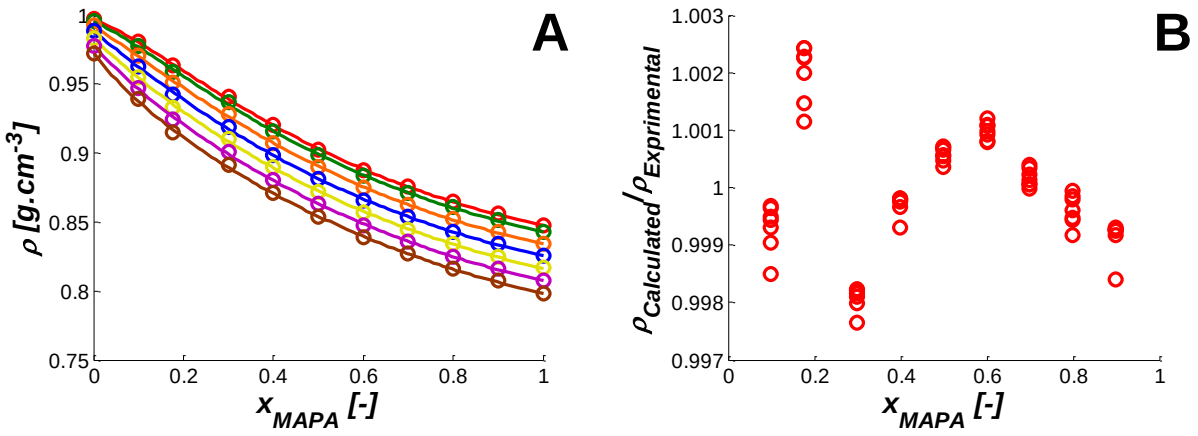

Figure 8: (A) Density for unloaded MAPA-water system. Experimental data: (**o**) from This Work. Temperatures: 298.15 K (Red), 303.15 K (Green), 313.15 K (Orange), 323.15 K (Blue), 333.15 K (Yellow), 343.15 K (Dark Pink), 353.15 K (Brown). (B) Ratio between calculated and experimental data for MAPA-water unloaded system.

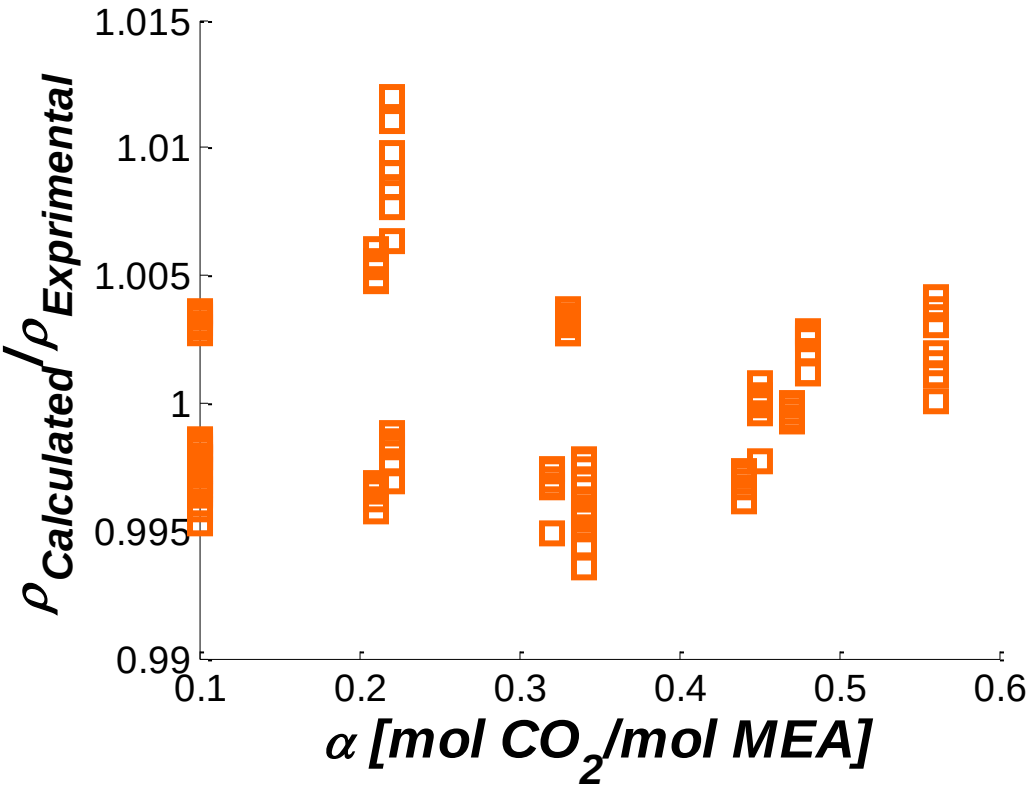

Figure 9: Ratio between the calculated and experimental densities for MEA loaded solutions. Proportionality model optimized using only data form Han et al. (2012b).

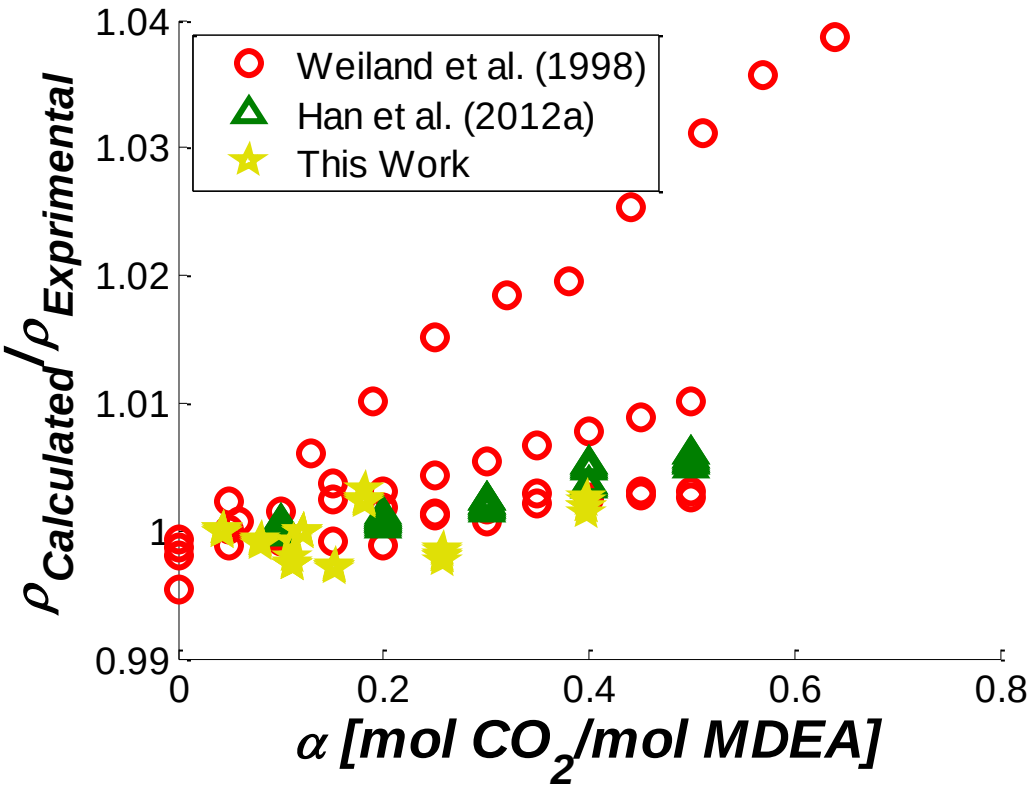

Figure 10: Ratio between the calculated and experimental densities for MDEA loaded solutions. Proportionality model optimized using only data form this work.

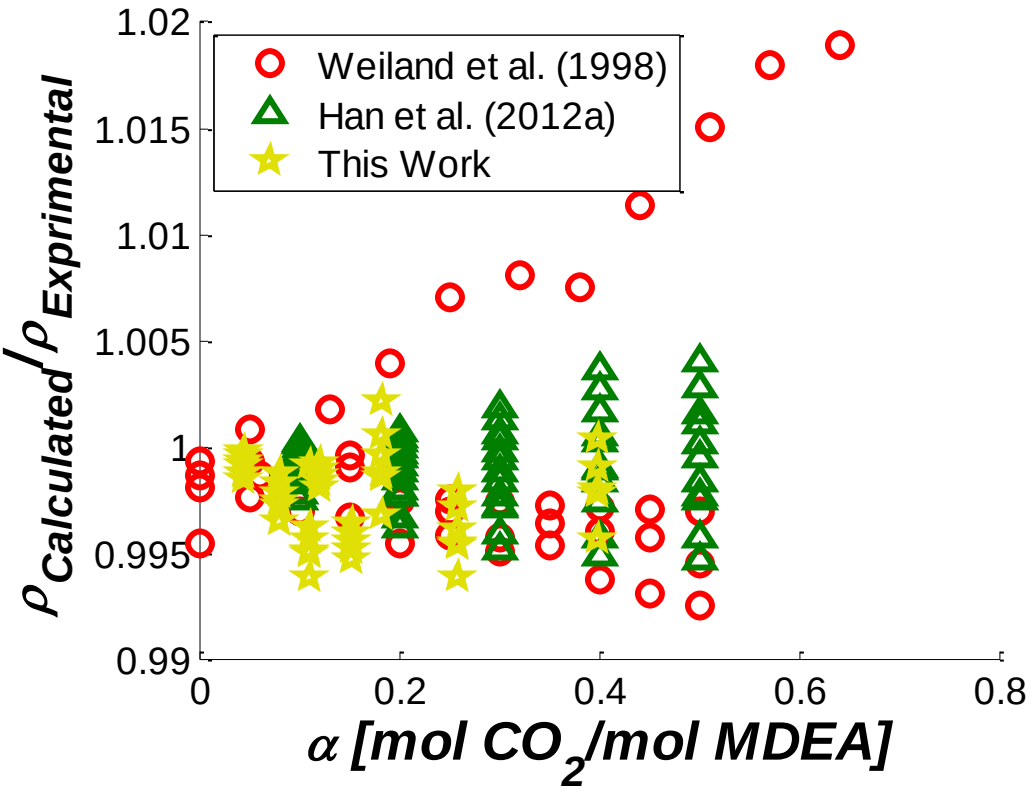

Figure 11: Ratio between the calculated and experimental densities for MDEA loaded solutions. Proportionality model optimized using data from Weiland et al. (1998), Han et al. (2012a) and this work.

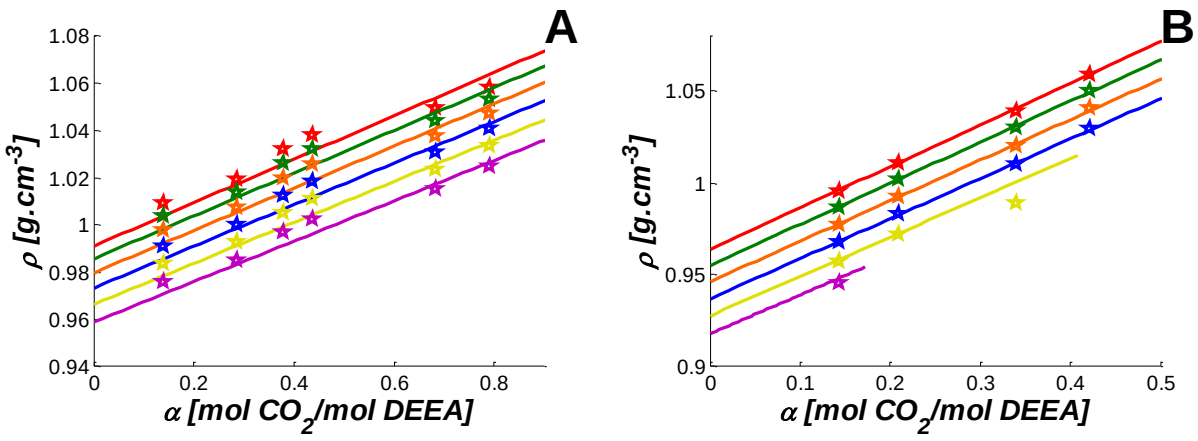

Figure 12: Calculated densities using the proportionality model for: (A) DEEA 24% mass and (B) DEEA 61% mass. Experimental data: (★) from This Work. Temperatures: 293.15 K (Red), 303.15 (Green), 313.15 K (Orange), 323.15 K (Blue), 333.15 K (Yellow), 343.15 K (Dark Pink).

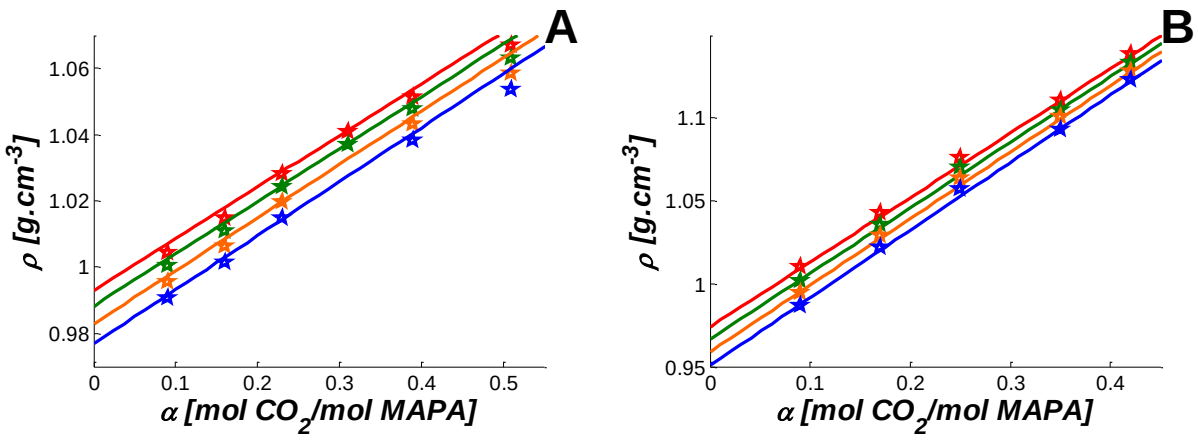

Figure 13: Calculated densities using the proportionality model for: (A) MAPA 18% mass and (B) MAPA 46% mass. Experimental data: (★) from This Work. Temperatures: 293.15 K (Red), 303.15 (Green), 313.15 K (Orange), 323.15 K (Blue).

Table 1: Literature data for unloaded and loaded solutions of MDEA, DMEA, DEEA and MEA considered in this work.

Amine	# of data	Temp. range [K]	Loaded	Source
MEA	74	298.15 – 318.15	No	Hawrylak et al. (2000)
	126	298.15 – 363.15	No	Han et al. (2012b)
	35	298.15 – 353.15	No	Amundsen et al. (2009)
	14	298.15	No	Touhara et al. (1982)
	40	303.15 – 318.15	No	Kapadi et al. (2002)
	119	298.15 – 363.15	Yes	Han et al. (2012b)
MDEA	126	298.15 – 353.15	No	Maham et al. (1995)
	78	298.15 – 318.15	No	Hawrylak et al. (2000)
	126	298.15 – 363.15	No	Han et al. (2012a)
	70	303.15 – 323.15	No	Chowdhury et al. (2009)
	44	298.15	Yes	Weiland et al. (1998)
	63	298.15 – 353.15	Yes	Han et al. (2012a)
DMEA	97	293.15 – 313.15	No	Zhang et al. (1995)
	66	298.15 – 318.15	No	Hawrylak et al. (2000)
DEEA	100	298.15 – 313.15	No	Zhang et al. (1995)
	80	298.15 – 318.15	No	Hawrylak et al. (2000)

Table 2: Amines studied in this work.

Amine	**Common name**	**Formula**	**CAS nr.**	**Purity (%) of the chemical used.**
MDEA	N-Methyldiethanolamine	$C_5H_{13}NO_2$	150-59-9	99
DMEA	N,N-Dimethylethanolamine	$C_4H_{11}NO$	108-01-0	99
DEEA	Diethylethanolamine	$C_6H_{15}NO$	100-37-8	99.5
MAPA	N-Methyl-1,3-diaminopropane	$C_4H_{12}N_2$	6291-84-5	98

Table 3: Coefficients for equation 20 describing the densities of pure solvents and water.

Chemical	$d_1 \cdot 10^6$	$d_2 \cdot 10^3$	d_3	AARD (%)	R^2	Data sources
Water	-3.3461	1.7296	0.77853	0.03	0.9997	Wagner and Pruß (2002)
MEA	-0.3544	-0.5765	1.2153	0.002	1.0000	Han et al. (2012b)
MDEA	-0.1992	-0.6399	1.2448	0.006	1.0000	This work
DMEA	-0.5500	-0.5133	1.0849	0.012	1.0000	This work
DEEA	-0.4852	-0.6322	1.1111	0.002	1.0000	This work
MAPA	-0.4013	-0.6323	1.0718	0.006	1.0000	This work

Table 4: Z^{RA} parameters and the calculated deviation for densities of pure amines.

	Z^{RA}	AARD (%)	R^2
WATER	0.24102	1.64	0.9997
MEA	0.24772	0.23	0.9999
MDEA	0.25323	0.28	0.9999
DMEA	0.26016	0.36	0.9998
DEEA	0.25949	1.69	0.9998
MAPA	0.27447	0.08	0.9999

Table 5: Regressed parameters for the Redlich-Kister (a_n and b_n) and the Rackett ($k_{H_2O\text{-}Amine}$) models for calculation of densities of unloaded amine solutions.

	a_1	b_1	a_2	b_2	a_3	b_3	$k_{H_2O\text{-}Amine}$
MEA	-3.5279	2.9445e-3	0.8791	-1.5892e-3	3.0507	-6.1863e-3	-0.033298
MDEA	-8.5036	1.2842e-2	5.8301	-1.0550e-2	4.7773e-1	-1.9200e-3	-0.01632
DMEA	-12.7738	2.0388e-2	5.7675	-0.8577e-2	2.2858	-9.0170e-3	0.002546
DEEA	-11.2847	1.2653e-2	6.6899	-1.2813e-2	-5.1906	8.7350e-3	0.020291
MAPA	-7.8636	-4.02e-3	10.4062	-2.1010e-2	-4.7552	1.4846e-2	0.13482

Table 6: Calculated deviations for the unloaded amine-water systems.

Amine	Source	AARD (%)		Max. deviation (kg/m^3)		Used in the regression?
		Redlich-Kister	Rackett[1]	Redlich-Kister	Rackett[1]	
MEA	Hawrylak et al. (2000)	0.06	0.62 (0.50)	2.16	16.50 (13.82)	No
	Han et al. (2012b)	0.02	0.50 (1.20)	0.73	21.88 (29.98)	Yes
	Amundsen et al. (2009)	0.04	0.54 (1.08)	0.91	16.49 (25.93)	No
	Touhara et al. (1982)	0.05	1.03 (0.44)	0.93	16.39 (12.95)	No
	Kapadi et al. (2002)	0.05	0.52 (0.50)	1.22	13.40 (12.45)	No
MDEA	Maham et al. (1995)	0.04	0.77 (0.85)	1.46	20.75 (31.11)	No
	Hawrylak et al. (2000)	0.08	0.69 (0.71)	2.29	16.54 (17.43)	No
	Han et al. (2012a)	0.06	0.83 (1.26)	1.95	24.80 (36.23)	No
	Chowdhury et al. (2009)	0.03	0.66 (0.71)	1.30	15.65 (18.62)	No
	This Work	0.03	0.75 (0.85)	1.61	20.87 (30.99)	Yes
DMEA	Zhang et al. (1995)	0.07	1.06 (0.92)	2.15	18.59 (16.74)	No
	Hawrylak et al. (2000)	0.09	0.81 (0.73)	1.97	17.04 (14.78)	No
	This Work	0.05	0.84 (0.86)	2.00	21.36 (25.96)	Yes
DEEA	Zhang et al. (1995)	0.05	1.04 (0.85)	1.46	19.04 (16.74)	No
	Hawrylak et al. (2000)	0.09	0.81 (0.70)	2.47	17.32 (16.64)	No
	This Work	0.06	0.95	1.54	23.61	Yes

			(1.03)		(27.45)	
MAPA	This Work	0.08	1.16 (1.40)	2.26	30.89 (27.48)	Yes

[1] The results in parenthesis are obtained if equation 13 is used for computing the binary interaction parameter, k_{ij}, instead of using the regressed values.

Table 7: Parameters for loaded systems.

Amine	Proportionality model parameters		Rackett parameter
	A	B	$k_{CO_2\text{-Amine}}$
MEA	0.7242	3.9713e-4	-8.1095
MDEA[1]	1.1081	-4.6456e-4	-8.9883
MDEA[2]	0.1167	2.3489e-3	-7.4335
DEEA	1.4793	-1.4617e-3	-6.7322
MAPA	0.9305	2.7899e-4	-18.9669

[1]Optimized using only this work's data.

[2] Optimized using data from Weiland et al. (1998), Han et al. (2012a) and this work.

Table 8: Deviations for loaded systems.

Amine	AAD [kg/m^3]		Max deviation [kg/m^3]		Source
	Proportionality	Rackett	Proportionality	Rackett	
MEA	3.4	9.04	12.6	20.0	Han et al. (2012b)
MDEA[1]	7.5	14.6	44.4	45.1	Weiland et al. (1998)
	2.6	6.2	6.4	19.2	Han et al. (2012a)
	1.6	7.7	3.4	25.1	This work
MDEA[2]	5.0	9.9	21.7	32.0	Weiland et al. (1998)
	1.8	8.3	5.8	21.8	Han et al. (2012a)
	2.6	7.9	6.5	28.0	This work
DEEA	3.3	19.2	11.5	34.0	This work
MAPA	2.0	14.3	6.3	34.0	This work

[1]Optimized using only this work's data.

[2] Optimized using data from Weiland et al. (1998), Han et al. (2012a) and this work.

Table A.1: Density for the unloaded aqueous MDEA solutions at different temperatures.

w_{MDEA}	x_{MDEA}	$\rho\ \left[g/cm^3\right]$					
		293.15 K	303.15 K	313.15 K	323.15 K	333.15 K	353.15 K
1.00000	1.00000	1.04012		1.02474	1.01727	1.00956	0.99394
0.98372	0.90136	1.04230		1.02698	1.01936	1.01154	0.99588
0.96479	0.80559	1.04413		1.02895	1.02127	1.01340	0.99761
0.94022	0.70398	1.04660		1.03142	1.02370	1.01582	0.99980
0.90799	0.59876	1.04952		1.03431	1.02655	1.01852	1.00235
0.87297	0.50961	1.05215		1.03694	1.02914	1.02116	1.00468
0.79939	0.37601	1.05634		1.04137	1.03358	1.02556	1.00887
0.75663	0.31979	1.05628		1.04126	1.03342	1.02540	1.00869
0.61559	0.19495	1.05298		1.03894	1.03152	1.02381	1.00755
0.50045	0.13156	1.04542	1.03964	1.03280	1.02594	1.01883	
0.41918	0.09840	1.03844		1.02696	1.02069	1.01391	0.99920
0.23616	0.04466	1.02027		1.01167	1.00654	1.00078	0.98776

Table A.2: Density for the unloaded aqueous DMEA solutions at different temperatures.

w_{DMEA}	x_{DMEA}	$\rho\ \left[g/cm^3\right]$					
		293.15 K	303.15 K	313.15 K	323.15 K	333.15 K	353.15 K
0.18168	0.04295	0.99297	0.98420	0.97898	0.97300	0.96682	0.95996
0.37989	0.11020	0.98758	0.97397	0.96662	0.95890	0.95066	0.94204
0.57130	0.21222	0.97216	0.95614	0.94761	0.93858	0.92912	0.91884
0.67903	0.29956	0.95786	0.94138	0.93261	0.92315	0.91334	0.90250
0.77045	0.40423	0.94240	0.92574	0.91694	0.90741	0.89752	0.88644
0.83075	0.49806	0.92946	0.91280	0.90392	0.89445	0.88456	0.87370
0.88024	0.59772	0.91884	0.90219	0.89326	0.88396	0.87416	0.86382
0.91860	0.69525	0.90861	0.89194	0.88293	0.87396	0.86408	0.85441
0.94891	0.78967	0.90096	0.88418	0.87530	0.86636	0.85662	0.84732
0.97986	0.90769	0.89274	0.87583	0.86714	0.85822	0.84929	0.83996
1.00000	1.00000	0.88716	0.87011	0.86162	0.85270	0.84420	0.83490

Table A.3: Density for the unloaded aqueous DEEA solutions at different temperatures.

w_{DEEA}	x_{DEEA}	$\rho\left[g/cm^3\right]$							
		293.15 K	293.15 K	303.15 K	313.15 K	323.15 K	333.15 K	343.15 K	353.15 K
0.05580	0.00900	0.99649		0.99366	0.98994	0.98544	0.98029	0.97450	0.96817
0.11820	0.02017	0.99524		0.99177	0.98744	0.98243	0.97679	0.97060	
0.23750	0.04566	0.99245		0.98721	0.98138	0.97499	0.96814	0.96087	
0.35820	0.07896	0.98647		0.97964	0.97246	0.96490	0.95698	0.94874	
0.41954	0.09993		0.97828	0.97457	0.96674	0.95873	0.95032	0.94153	0.93246
0.48160	0.12487	0.97668		0.96890	0.96077	0.95230	0.94362	0.93452	
0.61350	0.19602	0.96274	0.95775	0.95439	0.94555	0.93644	0.92705	0.91735	0.90602
0.61927	0.19987			0.95338	0.94458	0.93544	0.92600	0.91609	
0.73600	0.29983		0.94118	0.93669	0.92751	0.91797	0.90813	0.89779	0.88737
0.81040	0.39980		0.92814	0.92356	0.91422	0.90462	0.89465	0.88442	0.87392
0.86662	0.49979		0.91662	0.91200	0.90260	0.89304	0.88314	0.87301	0.86261
0.90685	0.59980		0.90699	0.90237	0.89307	0.88349	0.87365	0.86356	0.85373
0.93657	0.69983		0.89920	0.89466	0.88544	0.87588	0.86610	0.85612	0.84596
0.96290	0.79987		0.89124	0.88659	0.87737	0.86791	0.85821	0.84834	0.83830
0.98365	0.89993		0.88457	0.87997	0.87069	0.86125	0.85165	0.84191	0.83207
1.00000	1.00000		0.87947		0.86554	0.85612	0.84661	0.83703	0.82731

Table A.4: Density for the unloaded aqueous MAPA solutions at different temperatures.

w_{MAPA}	x_{MAPA}	$\rho\left[g/cm^3\right]$						
		298.15 K	303.15 K	313.15 K	323.15 K	333.15 K	353.15 K	363.15 K
0.35213	0.09990	0.98094	0.97743	0.97025	0.96283	0.95514	0.94717	0.93893
0.51216	0.17654	0.96339	0.95920	0.95065	0.94201	0.93315	0.92410	0.91486
0.67709	0.29981	0.94092	0.93662	0.92799	0.91915	0.91010	0.90089	0.89159
0.76537	0.39979	0.92042	0.91614	0.90748	0.89864	0.88960	0.88044	0.87130
0.83040	0.49995	0.90281	0.89851	0.88987	0.88101	0.87200	0.86288	0.85387
0.88023	0.60012	0.88763	0.88328	0.87465	0.86583	0.85692	0.84780	0.83895
0.91946	0.69982	0.87553	0.87120	0.86259	0.85372	0.84476	0.83572	0.82681
0.95140	0.79989	0.86499	0.86067	0.85189	0.84298	0.83405	0.82499	0.81652
0.97769	0.89947	0.85592	0.85167	0.84286	0.83404	0.82512	0.81607	0.80770
1.00000	1.00000	0.84764	0.84323	0.83433	0.82554	0.81668	0.80760	0.79840

Table A.5: Density of loaded solutions of aqueous MDEA solutions at different temperatures.

α	$\rho\left[g/cm^3\right]$					
	293.15 K	303.15 K	313.15 K	323.15 K	333.15 K	353.15 K
MDEA 23.8 mass %						
0.12	1.03275	1.02841	1.02355	1.01816	1.01218	
0.15	1.03860	1.03410	1.02919	1.02374	1.01763	
0.26	1.04703	1.04170	1.03734	1.03179	1.02533	1.01225
0.40	1.05543	1.04963	1.04553	1.03988	1.03347	
MDEA 50.0 mass %						
0.04	1.05348	1.04729	1.04072	1.03386	1.02660	1.01137
0.08	1.06134	1.05487	1.04851	1.04165	1.03440	1.01917
0.11	1.06892	1.06205	1.05602	1.04914	1.04182	1.02434
0.18	1.07672	1.06953	1.06375	1.05682	1.04954	1.03407

Table A.6: Density of loaded solutions of aqueous DEEA solutions at different temperatures.

α	$\rho\left[g/cm^3\right]$					
	293.15 K	303.15 K	313.15 K	323.15 K	333.15 K	343.15 K
DEEA 24.0 mass %						
0.14	1.00942	1.00394	0.99770	0.99094	0.98366	0.97596
0.29	1.01918	1.01371	1.00727	1.00026	0.99285	0.98492
0.38	1.03218	1.02621	1.01966	1.01252	1.00512	0.99690
0.44	1.03808	1.03214	1.02556	1.01840	1.01096	1.00262
0.68	1.04962	1.04401	1.03762	1.03074	1.02331	1.01532
0.79	1.05818	1.05312	1.04712	1.04073	1.03336	1.02468
DEEA 61.0 mass %						
0.14	0.99540	0.98656	0.97718	0.96784	0.95748	0.94530
0.21	1.01115	1.00220	0.99269	0.98316	0.97195	
0.34	1.03921	1.03024	1.02059	1.01043	0.98907	
0.42	1.05904	1.05026	1.04078	1.02976		

Table A.7: Density of loaded solutions of aqueous MAPA solutions at different temperatures.

α	$\rho\left[g/cm^3\right]$			
	293.15 K	303.15 K	313.15 K	323.15 K
MAPA 18.0 mass %				
0,09	1,00432	1,000355	0,995725	0,99054
0,16	1,01484	1,01095	1,006405	1,00131
0,23	1,02799	1,02412	1,019655	1,014695
0,31	1,04077	1,036975		
0,39	1,051425	1,047565	1,04322	1,03833
0,51	1,066755	1,06285	1,05847	1,05363
MAPA 46.0 mass %				
0,09	1,01009	1,00197	0,99448	0,98679
0,17	1,04259	1,03596	1,02911	1,02213
0,25	1,07590	1,06993	1,06373	1,05740
0,35	1,11028	1,10494	1,10076	1,09330
0,42	1,13847	1,13342	1,12812	1,12267